ECOGRAPHY

Research

When expansion stalls: an extension to the concept of range pinning in ecology

Thibaut Morel-Journel, Marjorie Haond, Laurent Lamy, David Muru, Lionel Roques, Ludovic Mailleret and Elodie Vercken

T. Morel-Journel (https://orcid.org/0000-0002-9124-2894) ✉ (thibaut.moreljournel@laposte.net), M. Haond, L. Lamy, D. Muru, L. Mailleret and E. Vercken, Univ. Côte d'Azur, INRAE, CNRS, ISA, France. – L. Roques, BioSP, INRA, Avignon, France. LM also at: Univ. Côte d'Azur, Inria, INRAE, CNRS, Sorbonne Univ., Biocore, France.

Identifying the factors modulating range expansion is essential to accurately predict changes in the spatial distribution of populations. By preventing population growth after dispersal, Allee effects can lead to front stops in discrete space, called 'pinning' if permanent. However, other mechanisms, such as positive density-dependent dispersal, have also been shown to affect the rate of range expansion and generate discrete-space front stops, albeit temporarily. In this study, we investigated the stability of the front stops generated by such mechanisms in relation to the carrying capacity of the environment. To this end, we performed artificial range expansions in discrete space using stochastic simulations and microcosm experiments. Simulation results confirmed that density-dependent dispersal alone can generate sustained front stops, albeit for a limited range of carrying capacities. We also highlighted the synergy between Allee effects and density-dependent dispersal on pinning emergence. Experimental results, obtained using a model species known to exhibit density-dependent dispersal, but without Allee effects, confirmed the model results. Furthermore, our study raises the issue of carefully considering the conditions for pinning stability, in a stochastic context and depending on the time-scale considered.

Keywords: allee effects, colonisation, density-dependent dispersal, microcosm, pinning, stochastic modelling

Introduction

Identifying the factors modulating range expansion is critical to accurately predict changes in the spatial distribution of populations. The dynamics of range shifts are complex and influenced by the interaction of multiple biotic and abiotic factors that affect population growth and dispersal through eco-evolutionary processes (Gaston 2009). Untangling these underlying factors and their respective effects is essential to the management of populations experiencing range shifts, whether they are invasive (Whitney and Gabler 2008, Tobin et al. 2011), affected by climate change

(Harley et al. 2006, Thomas 2010) or both (Kearney et al. 2008, Bellard et al. 2018).

Range expansion speed classically depends on the growth and dispersal of the populations on the edge of the range (called the 'front'). However, the colonisation speed can also be impacted by populations behind the front, through underlying demographic mechanisms (Stokes 1976, Roques et al. 2012, Birzu et al. 2018, Wang et al. 2019). This phenomenon is generally explained by Allee effects, i.e. positive relationships between individual fitness and population density occurring at low densities (Allee 1931, Courchamp et al. 2008). Allee effects can lead to negative growth rates under a given population size, referred to by Wang and Kot (2001) as the 'Allee threshold'. By driving new colonies ahead of the front to extinction, Allee effects can slow down range expansion.

Under specific conditions, expansion can even be stopped indefinitely. Keitt et al. (2001) coined the term 'pinning' to refer to propagation failures resulting in a stationary front, and also identified Allee effects as the underlying mechanism. In a discrete one-dimensional space of colonized habitat patches, except for a gap of extinct patches, Allee effects can prevent the colonisation of the gap without driving already existing populations to extinction. The range is therefore neither expanding nor contracting, but stationary in space. Keitt et al. (2001) also showed a correlation between the occupancy of neighbouring patches and the pinning stability: a patch's colonisation probability increased with the number of surrounding occupied patches, which act as sources of dispersal. This phenomenon, hereafter referred to as the 'neighbour effect', suggests a positive link between gap size and pinning stability. Most of the literature on invasion pinning stresses the need for strong Allee effects, with a positive Allee threshold, to observe stable invasion front stops over time (see Dowdall et al. 2018, Köhnke and Malchow 2019 and Wang et al. 2019 for recent examples) resulting in a range that can expand in pulses under certain conditions (Johnson et al. 2006).

However, other biotic and abiotic mechanisms can link expansion speed to the dynamics of populations behind the front (Bonnefon et al. 2014). One of them is positive density-dependent dispersal (Haond et al. 2018, Birzu et al. 2019), i.e. any monotonic increase in dispersal rate with population size, ranging from a linear increase to any part of a sigmoid function (Kun and Scheuring 2006, Altwegg et al. 2013) (Fig. 1). As the population size increases, the dispersal rate quickly reaches its maximum value for a concave function, while it remains very limited up to large population sizes for a convex one. The former is therefore expected to impede range expansion less than the latter (Altwegg et al. 2013). Sigmoid density dependent dispersal functions create threshold effects, with an intermediate population size separating low dispersal rates from high ones (Kun and Scheuring 2006, Parvinen et al. 2012). This threshold can generate temporary stops when dispersal is stochastic (Pachepsky and Levine 2011, Morel-Journel et al. 2016b). In this case, the dispersal rates from small populations on the front may be so low that
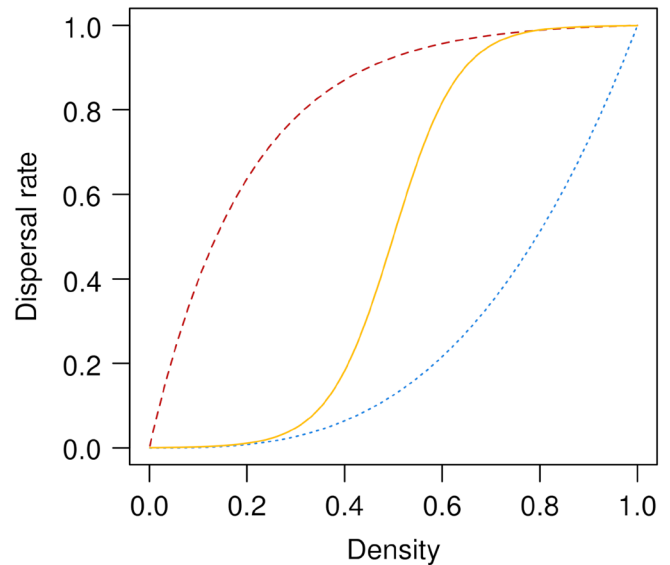

Figure 1. Examples of concave (red, dashed line), convex (blue, dotted line) or sigmoid (yellow, full line) density-dependence, represented as dispersal rates (in arbitrary units) as a function of density (in arbitrary units).

there is a high probability that no individual will disperse. Range expansion is then halted, until the density on the front is high enough to enable dispersal again. The existence of actual pinning, i.e. stable front stops, rather than temporary ones, remains to be explored.

In this study, we investigated the emergence of pinning in linear chains of populations at carrying capacity, except for a gap of empty patches, following Keitt et al. (2001). Using stochastic modelling of population dynamics, we showed that density-dependent dispersal alone could generate lasting stops in expansion, although only under specific conditions and for a limited range of carrying capacities. Besides, microcosm experiments using a minute wasp which exhibit positive density-dependent dispersal underlined the importance of the carrying capacity for the occurrence of range pinning generated by density-dependent dispersal. In light of these results, we proposed a new paradigm to study pinning and extinctions, based on a reversed point of view where extinction is seen as a colonization by an empty state. This gives new insight on the occurrence of pinning and extinction, depending on the gap size.

Material and methods

Computational model

We designed a stochastic model in discrete space and time with non-overlapping generations, which we used to simulate successively intra-patch dynamics (population growth in a single patch) and inter-patch dynamics (dispersal between patches) for each time step (Haond et al. 2018).

We drew the number of offspring after the intra-patch dynamics phase $O_{i,t}$ from a Poisson distribution defined as follows:

$$O_{i,t} \sim \text{Poisson}\left(R_{i,t}\ g(N_{i,t}) \right)$$

with $R_{i,t}$ the mean per capita growth rate in patch i at time t without Allee effects and $g(N_{i,t})$ the number of reproducing individuals in patch i at time t, potentially impacted by the Allee effects. We defined the mean per capita growth rate R_i according to a Ricker model:

$$R_{i,t} = e^{r\left(1 - \frac{N_{i,t}}{K}\right)}$$

with $N_{i,t}$ the population size in patch i at time t, r the exponential growth rate and K the carrying capacity (identical for every patch in the landscape). For simulations without Allee effects, the number of reproducing individuals $g(N_{i,t})$ was equal to $N_{i,t}$ the number of individuals in the patch i at time t. For simulations with Allee effects, we defined this number of reproducing individuals according to Haond et al. (2018), as follows:

$$g(N_{i,t}) = \begin{cases} N_{i,t}\ \dfrac{N_{i,t}}{\rho R_{i,t}} & \text{if } N_{i,t} \leq \rho R_{i,t} \\ N_{i,t} & \text{if } N_{i,t} > \rho R_{i,t} \end{cases}$$

with ρ the Allee threshold. Thus, we could separate the impact of the Allee effect (when $N_{i,t} \leq \rho R_{i,t}$) from the impact of the carrying capacity (when $N_{i,t} > \rho R_{i,t}$) on the growth rate.

We assumed isotropic dispersal within a one-dimensional stepping-stone landscape of n patches, with patches numbered in increasing order from 1 to n. We defined the number of individuals in patch i at time $t+1$ after the inter-patch dynamics phase as follows:

$$N_{i,t+1} = O^s_{i,t} + O^r_{i-1,t} + O^l_{i+1,t}$$

with $O_{i,t}{}^s$ the number of offspring in patch i at time t staying in the patch, $O^r_{i-1,t}$ the number of offspring in patch $i-1$ at time t dispersing to the right (i.e. to patch i) and $O^l_{i+1,t}$ the number of offspring in patch $i+1$ at time t dispersing to the left (i.e. to patch i). We drew the number of offspring from patch i at time t dispersing to the left $O_{i,t}{}^l$, to the right $O_{i,t}{}^r$ or not dispersing $O_{i,t}{}^n$ from a multinomial distribution as follows:

$$(O^l_{i,t}, O^n_{i,t}\ O^r_{i,t}) \sim \text{Multinomial}\left(O_{i,t}, p_1, p_0, p_1\right)$$

with p_0 the probability of not dispersing and p_1 the probability of dispersing either to the left or to the right. For the patches 1 and n with only one neighbour on the boundaries

of the landscape, $p_0 = 1 - p_1$. For the other patches with two neighbours, $p_0 = 1 - 2p_1$. For scenarios without density-dependent dispersal, the value of p_1 was equal to the constant p_{ind}. For scenarios with density-dependent dispersal, the value of p_1 was proportional to a Hill (1910) function (Fig. 2) and described as follows:

$$p_1(N_{i,t}) = p_{\max}\ \frac{N_{i,t}{}^\alpha}{\tau^\alpha + N_{i,t}{}^\alpha}$$

with τ the half saturation constant, α the shape parameter of the Hill function and $p_{\max} = \lim_{N \to \infty} p_1(N)$. With this formulation of density dependent dispersal, we were able to encompass both concave and sigmoid density-dependent dispersal functions, depending on the value of α (Fig. 2).

We fixed the value of $p_{\max}$ such that the probability p_1 with density-dependent dispersal was equal to p_{ind} when $N = N_{\text{ind}} = 2\tau$:

$$p_{\max} = p_{\text{ind}}\left(1 + \frac{1}{2^\alpha}\right)$$

Simulations

We used this model to simulate population dynamics, using the R software (<www.r-project.org>). We considered seven-patch landscapes, with two patches at carrying capacity on each borders and the three central patches left empty. We performed additional simulations in five-patch landscapes with a single patch as the central gap. The Supporting information presents these additional simulations. First, we performed
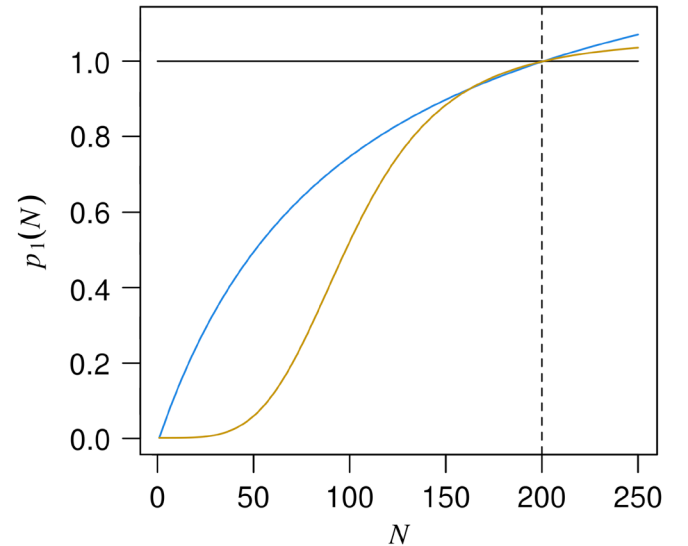

Figure 2. Value of $p_1(N)$ for $p_{\text{ind}} = 1$, $r = 0.2$, $\tau = 100$ and values of N between 1 and 250, without density-dependent dispersal (black), with density-dependent dispersal and $\alpha = 1$ (blue) or density-dependent dispersal and $\alpha = 4$ (yellow). The dashed lines correspond to $N = 2\tau$, i.e. the population size at which $p_1(N) = p_{\text{ind}}$.

simulations over 100 generations and for six scenarios, numbered from A to F. We simulated each scenario for 200×200 values of carrying capacity K between 1 and 200 and of maximum dispersal rate p_{ind} between 0.001 and 0.2, each repeated 100 times. Scenarios A, B and C did not include Allee effects, while scenarios D, E and F did, with $\rho = 20$. Scenarios A and D did not include density-dependent dispersal, scenarios B and E included a concave density-dependent dispersal function ($\tau = 100$, $\alpha = 1$) and C and F included a sigmoid density-dependent dispersal function ($\tau = 100$, $\alpha = 4$). All scenarios assumed $r = 0.2$.

We characterized each landscape after 100 generations either as 1) extinct if every patch in the landscape had a population size lower than $K/10$, 2) recolonised if every patch in the landscape had a population size greater than $K/10$ or 3) pinned otherwise. Besides, we defined 'pinning areas' in the two-dimensional planes of K and p_{ind} values. These areas comprised all the pairs of K and p_{ind} values for which more than 90% of the landscapes ended up pinned after 100 generations. We computed the size of these pinning areas as the number of different couples of values resulting in more than 90% of pinning over all the repetitions.

To assess the persistence of pinning in the landscapes on the long run, we also ran simulations for the scenarios with substantial pinning areas over 10 000 generations. To do so, we sampled 10 000 pairs of values of K and p_{ind} uniformly across the pinning areas, and performed simulations for each of them over 10 000 generations. Then, we recorded the values of K and p_{ind} for which landscapes were still pinned after 1, 10, 100, 1000 and 10 000 generations.

Microcosm experiments

In addition to the simulations, we performed experiments on microcosm stepping-stone landscapes using *Trichogramma chilonis* wasp as a model species. The landscapes were made-up of tubes (patches) linked to one another by pipes acting as pathways for the wasps to disperse freely. *T. chilonis* are oophagous parasitoids, generally used as biological control agents against various crop pests. They are especially suited to microcosm experiments, because of their small size and their short generation time. Besides, studies have shown that the Taiwan strain used in these experiments exhibits positive density-dependent dispersal in similar experimental designs (Morel-Journel et al. 2016b, Haond et al. 2018). During the experiment, we raised the wasps on eggs of *Ephestia kuehniella* irradiated beforehand, which prevented the emergence of caterpillars, without preventing the emergence of the wasps.

We manipulated two types of landscape features for the experiment. The carrying capacity of the patches was manipulated through the number of *E. kuehniella* eggs. We provided approx. 450 eggs each generation for the large carrying capacity treatment (noted 'K'), and 90 eggs for the small carrying capacity treatment (noted 'k'). The gap size was manipulated to assess the neighbour effect: either a small gap (a single empty patch, noted 'g') or a large gap (three empty patches, noted 'G'). Landscapes with a small gap were made up of five patches, while those with a large gap were made up of seven patches. G landscapes corresponded to the ones used for the simulations presented above. Overall, we considered three treatments for the experiment (Fig. 3): G/K (large carrying capacity and large gap), G/k (small carrying capacity and large gap) and g/k (small carrying capacity and small gap). To account for the stronger stochastic effects expected in smaller populations, we replicated the small carrying capacity treatments 16 times, and the large carrying capacity one 10 times. In order to correct for environmental heterogeneity, we distributed the replicates over four blocks and placed them into two rooms with regulated conditions (temperature: 20.5°C, humidity: > 70%, light period: 16 h), with a regular turnover.

We initiated the experiments by placing a number of parasitized eggs corresponding to the carrying capacity (90 or 450) in two patches on each border of the landscape (i.e. outside of the gap) and followed the dynamics for 9 generations. In the environmental conditions described above, each generation lasted for 14 days and was divided into two successive phases. First, adults were free to disperse through the pipes, mate and lay eggs during 48 h after emergence. Then, we removed adults and pipes in order to maintain non-overlapping generations and the larvae could develop during 12 days, until the next emergence. We provided new eggs three days before the scheduled emergence of adults, so that they were already available at the start of the next adult phase.
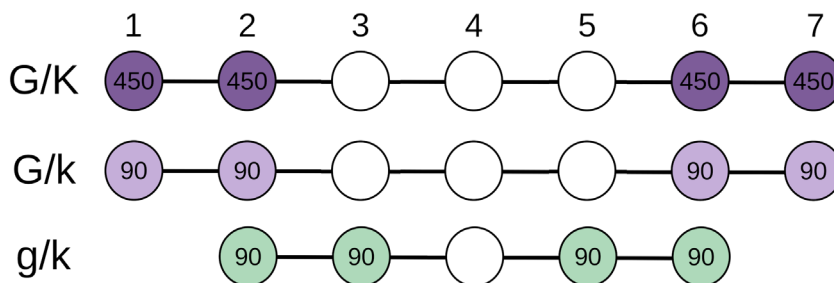

Figure 3. Schematic representation of the landscape used for the different treatments. They were initiated with two patches with either 90 (k) or 450 (K) individuals at each extremities of the landscapes, and a gap of either one (g) or three (G) empty patches in the middle. The patches are numbered from left to right and the colours for each landscape were attributed arbitrarily and are also used in Fig. 6.

We assessed population sizes by counting the number of parasitized eggs five days after the removal of adults, which turned turned black because of the chitinization of the *T. chilonis* pupae. Eggs were photographed for each generation and each replicate and population sizes were counted using the ImageJ software (Abràmoff et al. 2004). As for the simulations, we considered a patch as colonized if its population size was greater than 1/10th of the carrying capacity, and a landscape pinned if at least one of the patches in the gap was extinct.

Statistical analyses

We analysed the experimental results with generalized linear mixed-effects models (GLMM), using the R software (<www.r-project.org>) and the lme4 package (Bates et al. 2007). We assessed the impact of treatments on pinning at the level of the whole landscape with the proportion of empty patches in the gap and the time to first colonisation in the gap. The proportion of empty patches in the gap was computed at each generation and analysed using a logit link function. The GLMM used included the generation and the interaction between the generation and the experimental treatments as fixed effects, and the replicate as a random effect. Thus, we could investigate the impact of the treatment on the colonisation speed. We also computed the time to first colonisation as the number of generations before the first colonisation in the gap. It was therefore expected to follow a Poisson distribution and was analysed with a log link function. The GLMM used included the treatments as fixed effects and the experimental block as a random effect.

We assessed the neighbour effect by considering the first colonization of the edges of the gap, i.e. the patches 3 and 5 in the G landscapes and the patch 4 in the g landscapes, according to the numbering in Fig. 3. Firstly, we analysed the time to the first colonisation of each patch using a log link function. The GLMM used included the treatment as a fixed effect and the experimental block as a random effect.

Secondly, we considered the size of the source population the generation before the colonisation. In the G landscapes, the sources of the patches 3 and 5 were the populations in patches 2 and 6, respectively. In the g landscapes, the sources of the patch 4 were the populations in patches 3 and 5, respectively. For each source, we recorded the population size at the generation before the first colonisation in the corresponding patch of the gap. Therefore, two population sizes were recorded for each replicate, and analysed using a log link. The GLMM used included the treatment as a fixed effect and the replicate as a random effect.

Results

Medium-term simulations

The results of the simulations over 100 generations for the six scenarios are presented in Fig. 4. Every scenario exhibited an 'extinction area' (in grey) and a 'recolonisation area' (in blue), corresponding to pairs of parameter values for which most landscapes were respectively extinct and entirely recolonized after 100-time steps. All scenarios with Allee effects (D, E and F) also displayed a substantial pinning area (in yellow), but among those without Allee effects (A B and C), only the scenario with a sigmoid density-dependent dispersal function (C) did. Recolonisation always occurred for values of K and p_{ind} above a given threshold, and the lower boundary of the recolonisation area was systematically convex. Thus, recolonisation was always greatly facilitated by increasing both the carrying capacity K and the probability of dispersal p_{ind}. Complete extinction almost always occurred for values of K below a given threshold, which seems to be independent of p_{ind} in all scenarios except the one with Allee effects alone (D). In scenario D, increasing p_{ind} also increased the range of values of K leading to a total extinction of the landscape, up to $p_{ind} = 0.1$. In this scenario, the deterministic theory predicts that the threshold separating recolonisation and extinction is $K = 2\rho$ (Supporting information). Yet, demographic and dispersal stochasticity, coupled with the finite and discrete nature of the landscape considered, resulted in an increase in the threshold with the value of p_{ind}, up to $K = 54$.

When it existed, pinning systematically occurred between the recolonisation and extinction areas. Scenarios with either density-dependent dispersal (B and C) or with Allee effects (D) displayed different pinning dynamics. In scenario C in particular, pinning was mostly driven by the value of K, and mostly occurred for $15 < K < 35$, regardless of the value of p_{ind}. In scenario D however, pinning mostly occurred for low values of p_{ind}, but was less impacted by the value of K. The pinning areas of the scenarios including both Allee effects and density-dependent dispersal (E and F) included the pinning areas of scenarios with either mechanisms (B and D for scenario E, C and D for scenario F). However, the impacts seemed to reinforce each other. Indeed, there were combinations of parameter values for which none of the simulations with either mechanism (C and D) were pinned, whereas they were pinned for the scenario with both mechanisms (F). Overall, the pinning area for scenario F was 40% larger than the pinning areas for scenario C and D combined. Similarly, the pinning area for scenario E was 36% larger than the pinning areas for scenario B and D combined. The additional simulations performed in smaller landscapes with a gap of a single patch show similar pinning areas to those presented above. However, those areas are substantially smaller, with a reduction ranging from −44% for scenario F to −71% for scenario C. The results are presented in more details in the Supporting information.

Long-term simulations

We excluded scenario A and B from the simulations over 10 000 generations due to the very small size of their pinning areas. For the other scenarios, we only performed simulations with values of K and p_{ind} in the pinning area after 100 generations of each scenario. The results show different patterns
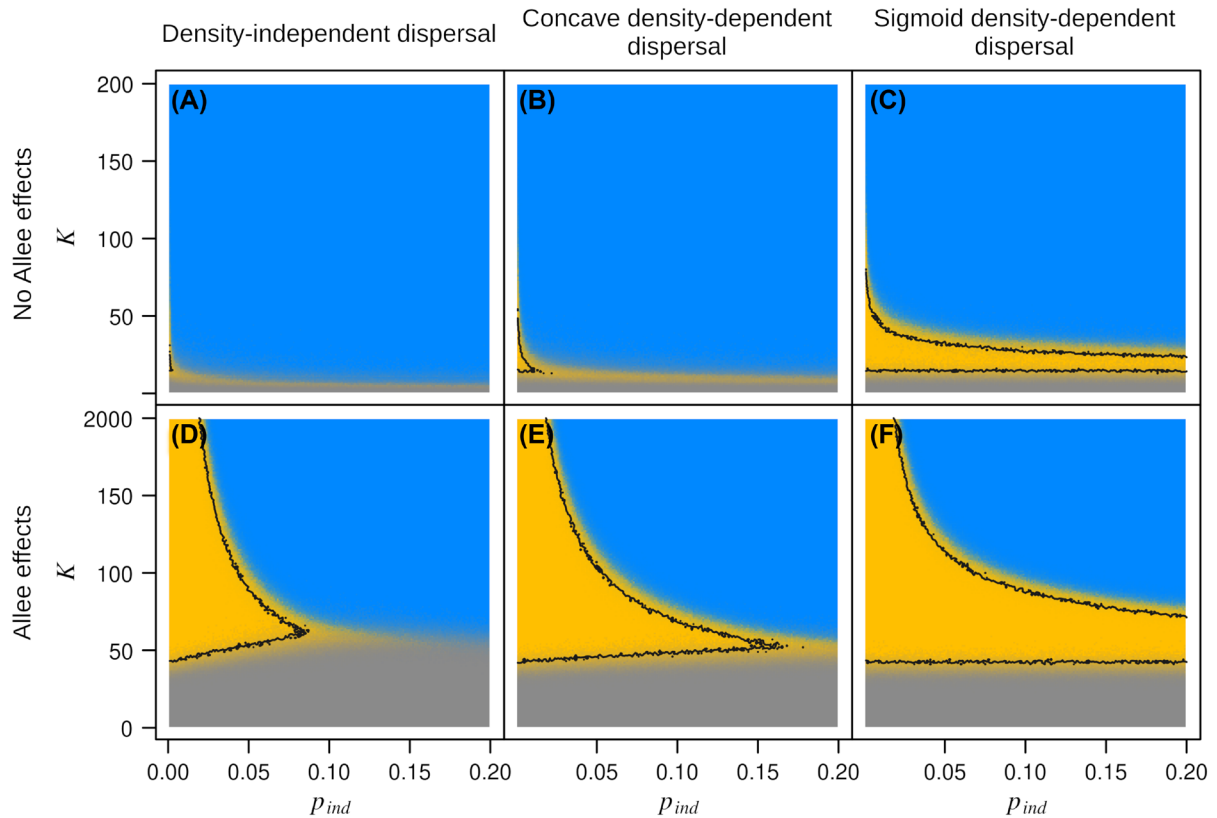
Figure 4. Status of the landscape after 100 generations of simulation for values of K between 2 and 200 and for values of p_{ind} between 0.002 and 0.2. (A), (B), (C) without Allee effects; (D), (E), (F) with Allee effects and $\rho = 20$; (A), (D) without density-independent dispersal; (B), (E) with density-dependent dispersal and $\alpha = 1$; (C), (F) with density-dependent dispersal and $\alpha = 4$. The colour of each pixel corresponds to the proportion of extinct (grey), recolonised (blue) and pinned (yellow) repetitions. The solid line delineates the repetitions for which more than 90% of the repetitions were pinned after 100 generations.

between the scenario without (C) and with Allee effects (D, E and F) (Fig. 5). As the result after 100 generations suggests, pinning was largely dependent on K for the scenario with density-dependent dispersal alone. The simulations exhibiting long-term pinning were all distributed along a curve going from $K = 38$ for $p_{ind} = 0.001$ to $K = 26$ for $p_{ind} = 0.02$ (Fig. 5C). Interestingly, this curve ran alongside the upper boundary of the pinning area after 100 generations. This means that simulated landscapes for scenario C with values around this upper boundary tended either to be recolonized after 100 generations, or remained pinned over very long time-frames.

Almost all simulations with Allee effects alone (D) exhibited long-time pinning for $K > 75$ and $p_{ind} < 0.02$. Beyond these values, the pinning duration gradually decreased towards the limits of the pinning area after 100 generations (Fig. 5D). The results concerning scenario E, combining Allee effects and concave density-dependent dispersal, were very similar to those for scenario D. The simulations including both Allee effects and sigmoid density-dependent dispersal exhibited both patterns observed for scenarios C and D. Yet, the strip of long-term pinning across all values of p_{ind} corresponded to higher values of K than in scenario C, and the upper boundary of the strip was well below the upper boundary of the pinning area.

Experimental results

The experimental results showed impacts of both the carrying capacity and the gap size on the stability of pinning. While all the G/k landscapes remained pinned over the course of the experiment, some with a higher carrying capacity (G/K) and those with a smaller gap (g/k) exhibited recolonisation during this period (Fig. 6). This was confirmed by the GLMM on the number of empty patches. As expected, the number of empty patches decreased with time $z = -13.13$, p < 0.0001). This decrease was faster in the G/K landscapes ($z = -11.72$, p < 0.0001) and in the g/k landscapes ($z = -3.25$, p = 0.001) than in the G/k ones. The time before the first colonisation was also significantly shorter with higher carrying capacity ($z = -3.67$, p = 0.0002), but not with a smaller gap ($p = 0.5120$).

When considering the colonization of the edges of the gap, increasing the carrying capacity also decreased the lag-time before the first colonisation ($z = -4.90$, p < 0.0001). Decreasing the gap size also tended to decrease the time to first colonisation, although the impact was not significant ($z = -1.84$, $p = 0.0653$). However, the population of the sources the generation before colonisation were smaller when the gap was smaller $z = -2.397$, $p = 0.0165$). This means that
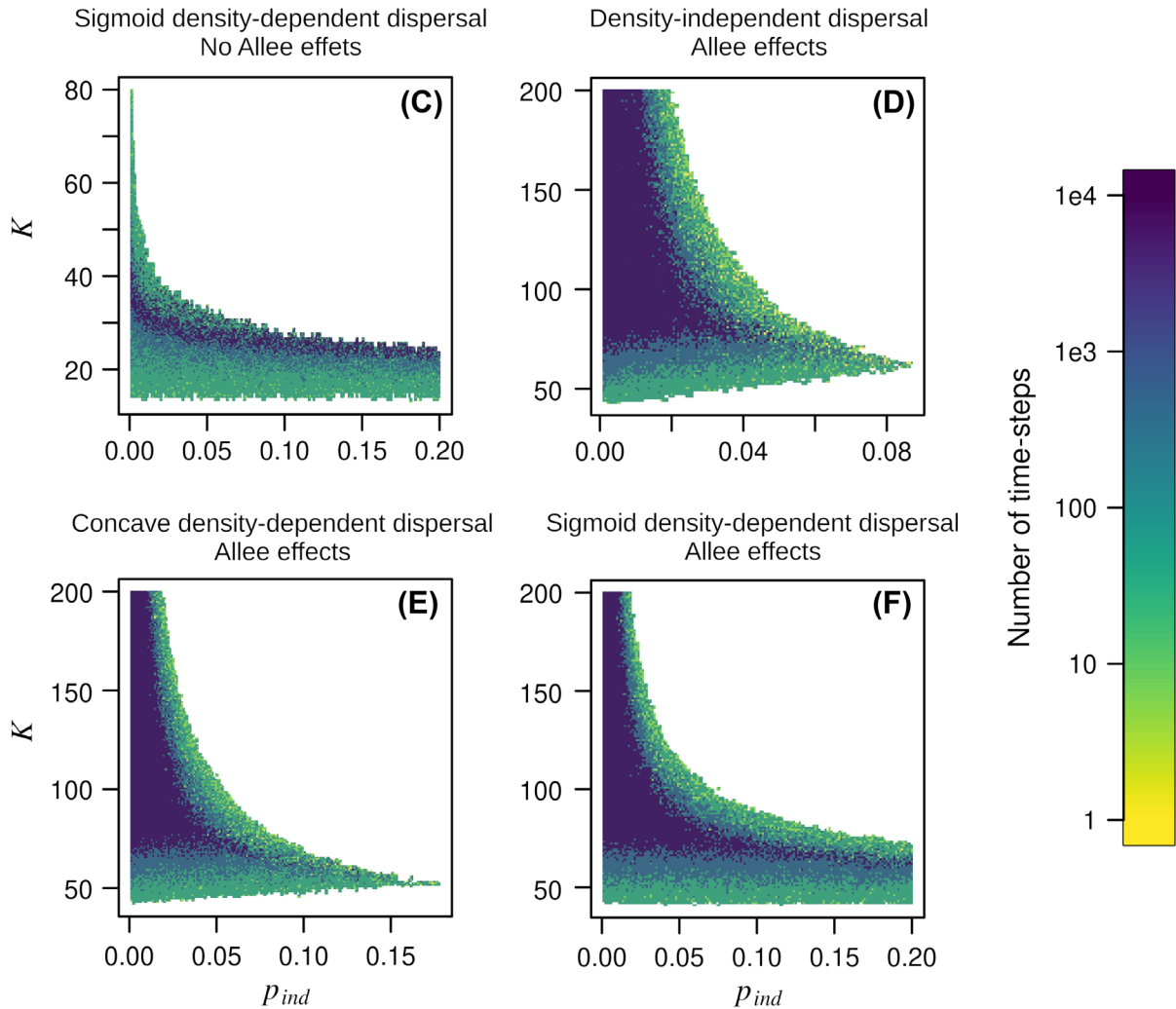
Figure 5. Duration (in log-scale) of the pinning for each couple of values of K and p_{ind} in the pinning area after 10 000 generations. (C) without Allee effects; (D), (E), (F) with Allee effects and $\rho = 20$; (D) with density-independent dispersal; E: with concave density-dependent dispersal ($\alpha = 1$); (C), (F) with sigmoid density-dependent dispersal ($\alpha = 4$). The scales of each figure of the panel were chosen to correspond to the most extreme values of the pinning areas for each scenario, and are therefore different from each other.

colonisation required smaller populations on the edge of the gap in the g/k landscapes compared to the G/k ones.

Discussion

This study shows that Allee effects are not systematically required to generate range pinning. Indeed our results indicate that density-dependent dispersal is sufficient, although for specific shapes of relationship between density and dispersal, and under specific conditions concerning the carrying capacity of the patches. This pinning was found to be stable over very long time periods (> 10 000 generations), although for more restricted parameter values than in simulations including Allee effects. Given our discrete simulations in time and space, pinning could occur in the absence of Allee effects if the dispersal rate was so low that either 1) no dispersing individuals were produced, or 2) the few

dispersing individuals failed to create a viable population due to demographic stochasticity. However, we cannot presume the existence of stable pinning in a continuous spatial or temporal context from these results. Previous studies showing front stops generated by density-dependent dispersal also considered a discrete landscape (Morel-Journel et al. 2016a, Wang et al. 2019), or fragmented landscapes with gap of inhospitable habitat (Pachepsky and Levine 2011). If pinning generated by density-dependent dispersal was possible in continuous landscapes, it would likely be unstable. This is the case for Allee effects according to Keitt et al. (2001), which also used discrete landscapes in their study.

Through simulations, we also demonstrated a synergy between Allee effects and density-dependent dispersal for the emergence of range pinning. Indeed, these mechanisms have different, but complementary impacts on colonisation. On the one hand, Allee effects do not prevent dispersal, but lead to reproduction failures when the number of dispersing
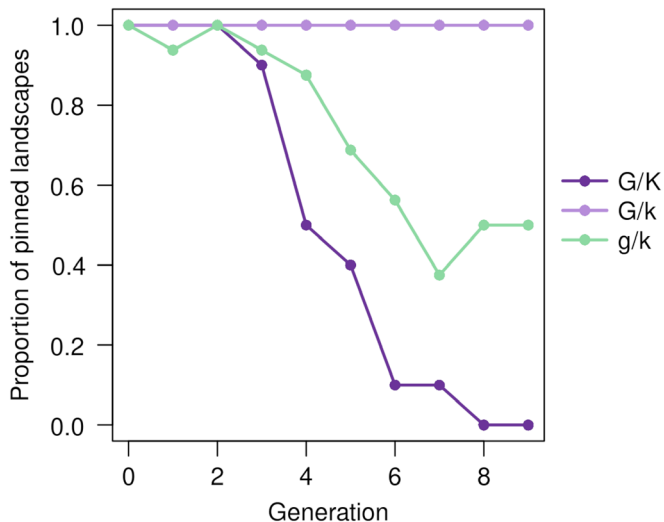
Figure 6. Proportion of pinned landscapes during the experiment over time, for the treatments G/K, G/k and g/k, defined as the proportion of landscapes in which at least one patch has a population size lower than $K/10$. The colours used correspond to those of Fig. 3.

individuals is below the Allee threshold. This is also why range pinning is not expected with weak Allee effects, which do not have a positive Allee threshold (Wang et al. 2019). On the other hand, density-dependent dispersal prevents dispersal, but cannot prevent any dispersing individual from successfully colonizing an empty patch. Together, these mechanisms prevent both dispersal and the reproduction of dispersing individuals, making the colonization of the whole landscape more difficult. In particular, density-dependent dispersal makes it more difficult to exceed the Allee threshold in newly colonized patches.

However, density-dependent dispersal also interacted with Allee effects in generating total extinctions. Provided dispersal fluxes are strong enough, emigration can deplete source populations and also drive them into the vortex of extinction created by Allee effects (Kanarek et al. 2013, Morel-Journel et al. 2016a). We observed this phenomenon in simulations with Allee effects alone, in which total extinction was more frequent with increased dispersal rates, up to $p_{ind} = 0.1$ (Fig. 4C). Total extinction occurred even for rather large values of K, because of the added impact of demographic stochasticity, which could randomly nudge existing populations below the Allee threshold. Yet, density-dependent dispersal maintained the size of small populations on the edges of the range above the Allee threshold by reducing their dispersal rate. By mitigating the deleterious impact of dispersal combined with Allee effects, density-dependent dispersal (especially sigmoid) prevented range contraction and overall extinction (Fig. 4E–F).

The impact of the carrying capacity on range pinning created by density-dependent dispersal was supported by both simulations and experiments. This is consistent with previous work showing that a correlation between the carrying capacity and range expansion speed was generated by Allee effects and positive density-dependent dispersal (Haond et al. 2018). In the simulations, its impact on pinning was also

conditioned by the shape of the density-dependent dispersal function. Indeed, pinning appeared for a given range of carrying capacities when using a sigmoid relationship between population size and dispersal rate, but not when using a concave one. While both functions were set to achieve a dispersal rate equal to p_{ind} for $N = 200$, the concave form led to a rapid increase at low densities. On the other hand, the sigmoid shape ensured that the actual dispersal rate remained small for densities below the inflection point (Fig. 2).

The Hill function used to describe the relationship between density and the dispersal rate was initially designed to represent dose-response relationships (Hill 1910), with a slope at the inflexion point becoming more marked as the value of α increases. If the carrying capacity was below this inflexion point, the range of achievable population sizes was entirely in the lower part of the sigmoid, drastically limiting dispersal.

For instance, pinning mostly occurred for $K < 40$ in scenario C (Fig. 4C), i.e. for populations remaining small, below the inflexion point, at $N = 88$ (Fig. 2). A similar effect is expected for carrying capacities below the Allee threshold, but on growth rate rather than dispersal. Indeed, setting a carrying capacity below the Allee threshold ($K < \rho$) leads to negative growth rates in each population because of Allee thresholds. This ensured complete extinction for every simulation with $K \leq 20$ and Allee effects (Fig. 4D–F).

Even though the experiments only lasted for ten generations, results also showed the impact of the carrying capacity on the speed at which the gap was recolonized. Notably, all G/K landscapes were recolonised during the experiment, but none of the G/k landscapes were. The carrying capacity also reduced the duration of the lag before any colonisation began in the gap, both in the landscape as a whole and in patches at the edge of the gap. This result confirms that limiting the carrying capacity – and thus the size of the populations providing dispersing individuals – increased the chances that no dispersal occurred.

Our simulation results support the neighbour effect (Supporting information). Indeed, reducing the size of the gap allowed for recolonization rather than pinning, for a number of parameter combinations. This was the case for scenarios including Allee effects, as expected according to Keitt et al. (2001), but also in presence of density-dependent dispersal. Yet, this impact of gap size was not as clear-cut in our experimental results. Indeed, there was no difference between the g/k and the G/k landscapes in the time to first colonisation in the gap, and results concerning the patches on the edges of the gap did not bring strong evidence for a neighbour effect either. Those patches tended to be colonized faster in g/k landscapes compared to the G/k ones, but there was no significant difference. However, our results also indicate that the sizes of the source populations required to colonize an empty patch were smaller if there was more of them. This suggests that increasing the number of neighbouring populations compensated for their smaller size, and enabled colonization despite the density-dependent dispersal. A lack of statistical power in our analyses could explain why this effect does not clearly result in a neighbour effect.

We were able to investigate the neighbour effect by using the same landscape structure as Keitt et al. (2001), i.e. a linear chain of populations at carrying capacity, except for a gap. In this framework, every patch of the landscape initially belongs to one of two states – either occupied or empty – and the structure corresponds to a contiguous set of empty patches in a landscape of occupied patches. Interestingly, this setup mirrors the initial landscape structure encountered in invasions, i.e. a set of occupied patches in a landscape of empty patches. From this observation, we argue that the dynamics of pinning can be modelled as an 'invasion' of the occupied state by an empty one, the same way as classical invasions of the empty state by the occupied one (Supporting information). Namely, instead of focusing on the dynamics of a population density, we propose to focus on the dynamics of the unoccupied space. From this viewpoint, pinning is akin to the 'establishment' of the empty state in an occupied landscape. Our computations in the Supporting information show that this point of view can be readily applied to standard reaction-diffusion models with a strong Allee effect, as those considered e.g. in Lewis and Kareiva (1993). Therefore, we argue that the literature on the conditions for successful invasion provides insight on the conditions for pinning stability. In particular, basing ourselves on the known results about the minimum patch size for invasion, we proved in the Supporting information that, in the reaction-diffusion framework, there exists a critical gap size delimiting complete recolonisation from complete extinction and pinning. This is consistent with our simulation results. Using this perspective, we can foresee the complex interplay between pinning, extinction and spatial distribution of the gaps. For instance, we expect that depending on their respective positions, two gaps may increase or decrease the chances for pinning and extinction, compared to a single gap of the same size (Supporting information).

For this study, we had to consider a definition of pinning accounting for stochastic dynamics. In this context, the stability of pinning can only be relative, as the only perfectly stable state of the landscape is the complete extinction of each patch. Indeed, the probability of extinction of a population is never zero, whatever its size, nor is the probability of recolonisation of an empty patch, provided that there is at least one population in the landscape and that dispersal is possible. For the simulations, we defined stability as the persistence of pinning over extensive time frames. Pinning over 100 generations was already very long compared to the size of the landscape (seven patches) and of the gap to colonize (three patches). Pinning over 10 000 generations in this type of landscape could therefore be considered as extremely stable. Similarly, we could not observe permanent front stops in the experimental invasions, which are also stochastic processes (Melbourne and Hastings 2009). In particular, the pinning observed in the G/k landscapes would probably have disappeared if the experiment had lasted more than 10 generations.

More generally, these results highlight the need to be mindful of the time scale when considering pinning. Beside stochastic effects, pinning stability relies on specific environmental conditions and biological mechanisms, which can themselves vary over time. Variations in the carrying capacity of the environment – which impacts pinning stability – can be mitigated by the rather short timespan of biological invasions. Evolution however, can occur during the course of the invasion, notably with regard to Allee effects (Erm and Phillips 2020, Alfaro et al. 2021) or to the relationship between density and dispersal (Kun and Scheuring 2006, Travis et al. 2009, Dahirel et al. 2021). Therefore, pinning is likely to be observed in real range expansions, but the time scales on which it is stable may be limited by variations in the conditions required for its emergence.

While pinned range expansions are generally linked to strong Allee effects, we showed in this study that they can also be driven by density-dependent dispersal. Whatever the mechanism considered, pinning seemed to strongly depend on the carrying capacity of the environment, through its impact on the size that can be reached by populations at the edge of their range. Our experimental results using a species experiencing density-dependent dispersal confirmed this link with carrying capacity, which is consistent with the more general link between carrying capacity and range expansion speed in the presence of these mechanisms. Therefore, the existence of pinning for other factors linking them to one another (e.g the presence of competitor species or climate constraints, as listed by Bonnefon et al. 2014) could also be investigated. Our results in a stochastic context also shed light on the definition of pinning itself, especially with respect to its stability over time. In particular, considering a continuous scale of the stability of front stops relative to the considered time frame might be more relevant in a real life context than a dichotomy between pinned and expanding populations.

Author contributions

Thibaut Morel-Journel: Formal analysis (lead); Software (lead); Visualization (lead); Writing – original draft (lead). **Marjorie Haond**: Conceptualization (equal); Funding acquisition (supporting); Methodology (lead); Software (supporting); Writing – original draft (supporting). **Laurent Lamy**: Investigation (equal); Writing – original draft (supporting). **David Muru**: Investigation (equal); Writing – original draft (supporting). **Lionel Roques**: Conceptualization (equal); Supervision (equal); Writing – original draft (equal). **Ludovic Mailleret**: Conceptualization (equal); Formal analysis (supporting); Funding acquisition (equal); Software (supporting); Supervision (equal); Writing – original draft (equal). **Elodie Vercken**: Conceptualization (equal); Formal analysis (supporting); Funding acquisition (equal); Software (supporting); Supervision (equal); Writing – original draft (equal).

References

Abràmoff, M. D. et al. 2004. Image processing with ImageJ. – Biophotonics Int. 11: 36–42.

Alfaro, M. et al. 2021. When the Allee threshold is an evolutionary trait: persistence vs. extinction. – J. Math. Pures Appl. 155: 155–191.

Allee, W. C. 1931. Animal aggregations, a study in general sociology. – Univ. of Chicago Press.

Altwegg, R. et al. 2013. Density-dependent dispersal and the speed of range expansions. – Divers. Distrib. 19: 60–68.

Bates, D. et al. 2007. The lme4 package. – R package ver. 2: 74. <https://cran.r-project.org/web/packages/lme4/>.

Bellard, C. et al. 2018. Insights from modeling studies on how climate change affects invasive alien species geography. – Ecol. Evol. 8: 5688–5700.

Birzu, G. et al. 2018. Fluctuations uncover a distinct class of traveling waves. – Proc. Natl Acad. Sci. USA 115: E3645–E3654.

Birzu, G. et al. 2019. Genetic drift in range expansions is very sensitive to density dependence in dispersal and growth. – Ecol. Lett. 22: 1817–1827.

Bonnefon, O. et al. 2014. The spatio-temporal dynamics of neutral genetic diversity. – Ecol. Complex. 20: 282–292.

Courchamp, F. et al. 2008. Allee effects in ecology and conservation. – Oxford Univ. Press.

Dahirel, M. et al. 2021. Shifts from pulled to pushed range expansions caused by reduction of landscape connectivity. – Oikos 130: 708–724.

Dowdall, J. et al. 2018. Invasion pinning in a periodically fragmented habitat. – J. Math. Biol. 77: 55–78.

Erm, P. and Phillips, B. L. 2020. Evolution transforms pushed waves into pulled waves. – Am. Nat. 195: E87–E99.

Gaston, K. J. 2009. Geographic range limits of species. – Proc. R. Soc. B 276: 1391–1393.

Haond, M. et al. 2018. When higher carrying capacities lead to faster propagation. – bioRxiv 307322, ver. 4 peer-reviewed and recommended by Peer Community in Ecology.

Harley, C. D. et al. 2006. The impacts of climate change in coastal marine systems. – Ecol. Lett. 9: 228–241.

Hill, A. V. 1910. The possible effects of the aggregation of the molecules of haemoglobin on its dissociation curves. – J. Physiol. 40: 4–7.

Johnson, D. M. et al. 2006. Allee effects and pulsed invasion by the gypsy moth. – Nature 444: 361–363.

Kanarek, A. R. et al. 2013. Allee effects, aggregation and invasion success. – Theor. Ecol. 6: 153–164.

Kearney, M. et al. 2008. Modelling species distributions without using species distributions: the cane toad in Australia under current and future climates. – Ecography 31: 423–434.

Keitt, T. H. et al. 2001. Allee effects, invasion pinning and species' borders. – Am. Nat. 157: 203–216.

Köhnke, M. and Malchow, H. 2019. Wave pinning in competition–diffusion models in variable environments. – J. Theor. Biol. 461: 204–214.

Kun, Á. and Scheuring, I. 2006. The evolution of density-dependent dispersal in a noisy spatial population model. – Oikos 115: 308–320.

Lewis, M. A. and Kareiva, P. 1993. Allee dynamics and the spread of invading organisms. – Theor. Popul. Biol. 43: 141–158.

Melbourne, B. A. and Hastings, A. 2009. Highly variable spread rates in replicated biological invasions: fundamental limits to predictability. – Science 325: 1536–1539.

Morel-Journel, T. et al. 2016a. Evidence for an optimal level of connectivity for establishment and colonization. – Biol. Lett. 12: 20160704.

Morel-Journel, T. et al. 2016b. The highs and lows of dispersal: how connectivity and initial population size jointly shape establishment dynamics in discrete landscapes. – Oikos 125: 769–777.

Morel-Journel, T. et al. 2021. Data from: When expansion stalls: an extension to the concept of range pinning in ecology. – Dryad Digital Repository, <https://doi.org/10.5061/dryad.0zpc866zk>.

Pachepsky, E. and Levine, J. M. 2011. Density dependence slows invader spread in fragmented landscapes. – Am. Nat. 177: 18–28.

Parvinen, K. et al. 2012. Evolution of complex density-dependent dispersal strategies. – Bull. Math. Biol. 74: 2622–2649.

Roques, K. et al. 2012. Allee effect promotes diversity in traveling waves of colonization. – Proc. Natl Acad. Sci. USA 109: 8828–8833.

Stokes, A. 1976. On two types of moving front in quasilinear diffusion. – Math. Biosci. 31: 307–315.

Thomas, C. D. 2010. Climate, climate change and range boundaries. – Divers. Distrib. 16: 488–495.

Tobin, P. C. et al. 2011. Exploiting Allee effects for managing biological invasions. – Ecol. Lett. 14: 615–624.

Travis, J. M. et al. 2009. Accelerating invasion rates result from the evolution of density-dependent dispersal. – J. Theor. Biol. 259: 151–158.

Wang, C.-H. et al. 2019. Pinned, locked, pushed and pulled traveling waves in structured environments. – Theor. Popul. Biol. 127: 102–119.

Wang, M.-H. and Kot, M. 2001. Speeds of invasion in a model with strong or weak Allee effects. – Math. Biosci. 171: 83–97.

Whitney, J. D. and Gabler, C. A. 2008. Rapid evolution in introduced species, 'invasive traits' and recipient communities: challenges for predicting invasive potential. – Divers. Distrib. 14: 569–580.